**Separation Science and Technology**
Publication details, including instructions for authors and subscription information:
http://www.informaworld.com/smpp/title~content=t713708471

# Adsorption Characteristics of Propylene on Molecular Sieve 4A

Katsuyuki Kubota[a]; Kenji Nakajima[a]; Yoshinobu Ono[a]; Shinya Hayashi[a]
[a] Department of Chemical Engineering, The Faculty of Engineering Kobe University Nada-Ku, Kobe, Japan

**To cite this Article** Kubota, Katsuyuki , Nakajima, Kenji , Ono, Yoshinobu and Hayashi, Shinya(1989) 'Adsorption Characteristics of Propylene on Molecular Sieve 4A', Separation Science and Technology, 24: 9, 709 — 719
**To link to this Article: DOI:** 10.1080/01496398908049803
**URL:** http://dx.doi.org/10.1080/01496398908049803

SEPARATION SCIENCE AND TECHNOLOGY, 24(9&10), pp. 709-719, 1989

# Adsorption Characteristics of Propylene on Molecular Sieve 4A

KATSUYUKI KUBOTA, KENJI NAKAJIMA, YOSHINOBU ONO, and SHINYA HAYASHI

DEPARTMENT OF CHEMICAL ENGINEERING
THE FACULTY OF ENGINEERING
KOBE UNIVERSITY
NADA-KU 657, KOBE, JAPAN

## Abstract

Instead of the previous conventional experimental techniques for the measurement of the adsorption isotherm on a gas–solid system, a technically simple and convenient method is presented. Studies on the adsorption of propylene gas on molecular sieve 4A pellets were carried out. The amount of heat generated during the course of the adsorption and the effective diffusion coefficient of propylene gas was estimated and measured, respectively. By plotting the diffusion coefficient in the form of the Arrhenius correlation, the adsorption energy was evaluated. As a result, the magnitude of the energy was found to be reasonable in the light of that reported by other investigators, and further the correlation did not depend on the pellet sizes, suggesting that micropore diffusion was predominant to mass transfer limiting processes within the pellet.

## EXPERIMENTAL

The schematic flow diagram of the experimental apparatus is shown in Fig. 1. Pure propylene and helium gases with known flow rates were mixed in the mixing chamber filled with glass wool. Each flow rate was measured by the rotameter. The mixed gas was fed into the eight-way valve and led to the copper U-tube adsorbent holder which contains the spherical molecular sieve 4A pellets. The mixed gas was led to the sample

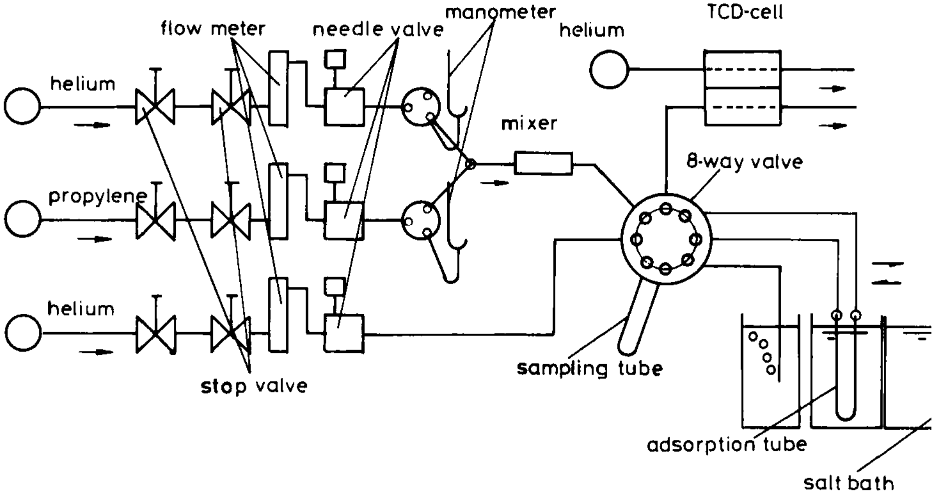

FIG. 1. The schematic diagram of the present experimental apparatus.

side of the thermal conductivity cell (TCD cell) kept at the constant temperature of 343.2 K, while a helium gas stream was led to the reference side. The completion of dynamical adsorption was ascertained by stabilizing the bridge balance of the TCD cell. After adsorption was completed, the adsorption holder was immersed in another salt bath, kept at a higher temperature (about 573 K), and, in doing so, rapid desorption was achieved. The desorbed adsorptive species was carried with the stream of the dissolution carrier gas into the reference side of the cell by way of the eight-way valve as shown in Fig. 1.

The area of each curve on the recorder chart was compared with that of a known amount of pure propylene gas, and the amount of the adsorptive species at a certain mole fraction and temperature was determined. The calibration line for the comparison was obtained by use of sampling tubes of different volumes. The concentration of the adsorptive species in the carrier was estimated from the readings of the flowmeters as shown in Fig. 1. The distance between the salt bath and the inlet of the cell was about 2 m, enough to attain a stable temperature of 343.2 K for the cell.

## EXPERIMENTAL RESULTS AND DISCUSSION

The experimental isotherms are shown in Fig. 2. The adsorbed amount of the component of interest is correlated against its concentration. The

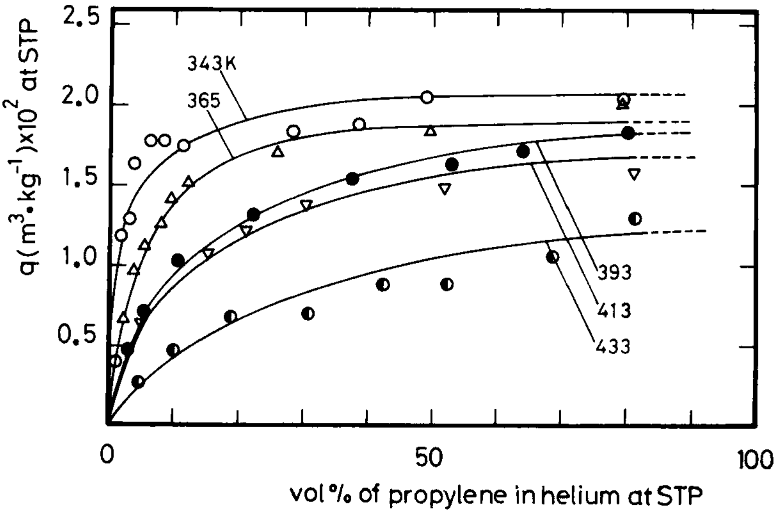

FIG. 2. The experimental adsorption isotherms of the pure propylene gas-molecular sieves 4A system.

adsorption densities are reduced to the standard state. The isotherm curves tend to increase with a decrease in temperature and an increase in concentration, and each curve tends to level-off at a maximum value. According to previous work (*1*), Langmuir's forward adsorption rate constant and the forward rate are given by

$$k_2 = (Ncs_0 \exp(-E_a^*/RT))/(2\pi MRT)^{1/2} \tag{1}$$

$$R_a = k_2(1-\theta)C \tag{2}$$

while Langmuir's backward desorption rate constant and the backward rate are given by

$$k_1 = (1/\tau_0)\exp(-E_d^*/RT) \tag{3}$$

$$R_d = k_1\theta \tag{4}$$

Here the relationship $E_d^* = E_a^* + Q$ holds. $E_a^*$, $E_d^*$, and $Q$ are the activation energy of adsorption, the activation energy of desorption, and the adsorption energy, respectively. In the equilibrium state, Eq. (5) can be derived:

$$k_2(1 - \theta)C = k_1\theta \tag{5}$$

By considering the relationship $\theta = q/q_{\mathrm{max}}$, Langmuir's correlation can be described by

$$C/q = (1/bq_{\mathrm{max}}) + (C/q_{\mathrm{max}}) \tag{6}$$

$b$ is equal to the ratio $k_2/k_1$, and can be given by Eq. (7), where it can be seen that $b$ is a weak function of the absolute temperature:

$$\begin{aligned} b &= k_2/k_1 \\ &= (Nc\sigma_0/(2\pi MRT)^{1/2})/((1/\tau_0)\exp(-Q/RT)) \\ &= b_0\,(\text{at a reference temperature})\exp(Q/RT) \end{aligned} \tag{7}$$

By plotting $C/q$ against $C$, one can estimate the maximum adsorption density of each curve and $b$, which varies theoretically with the function $T^{1/2}$. By taking this weak temperature dependency on $b$ into account, the modified $b$ for each temperature was calculated. By using this $b$, the recalculated curves are obtained. They are shown by the dashed curves in Fig. 3, together with the original data. The experimental curves seem to be supported by the calculated ones, although discrepancies are observed at 343 and 393 K.

The adsorption energy $Q$ can be estimated from Eq. (7) by correlating $b$ against $1/T$ on a semilogarithmic scale, which resembles the Arrhenius correlation. The plots obtained are shown in Fig. 4, and it can be seen that a linear correlation is obtained, and the amount of the energy of adsorption is estimated as $Q = 31$ kJ/mol. We suspect that the present system is a region of physical adsorption (*1*). Previously, Ruthven, Garg, and Crawford (*2*) reported an adsorption energy of 41.9 kJ/mol for their propylene–molecular sieve 5A system where the experiments were carried out by the weighing method. A straightforward discussion on this discrepancy cannot be given because their crystal pore radius was different from that of the present work. However, the present work's value is reasonable.

We have also investigated the effective diffusion coefficient or the apparent diffusion coefficient for the adsorptive species diffusing into the pellet or from it. The measurement was based on a sort of stepwise concentration response method. From the material balance with respect to the adsorptive component at any time and distance of a pellet, Eq. (8) can be derived (*3*):

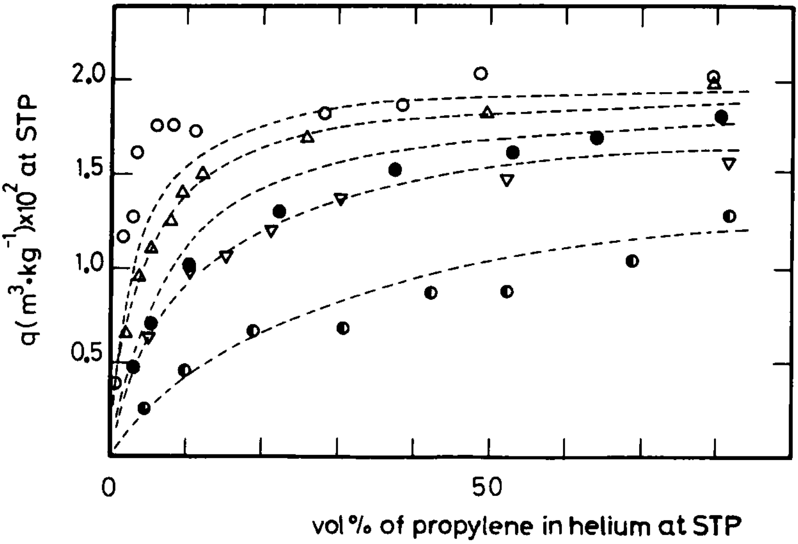

FIG. 3. The comparison of the recalculated isotherms with the observed ones.

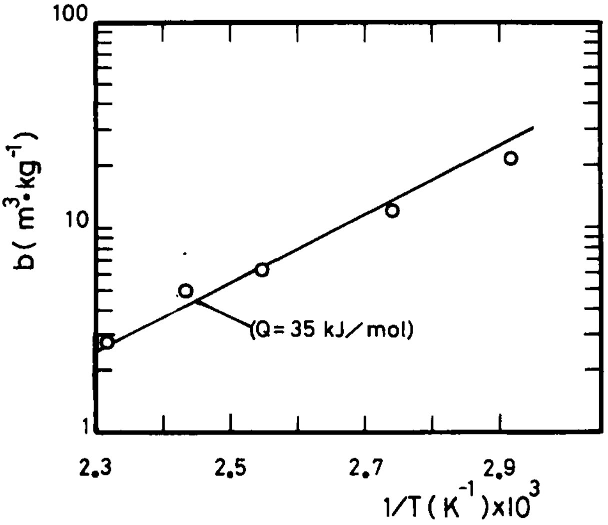

FIG. 4. The plots for estimating the adsorption energy.

$$\partial q/\partial t = (D_{app}/\rho^2)\partial/\partial\rho(\rho^2\partial q/\partial\rho) \tag{8}$$

The present experimental boundary conditions for this equation are as follows:

$$q(\rho,0) = Q_0; \qquad \partial q/\partial\rho(0,t) = 0; \qquad q(a,t) = q_s = 0 \tag{9}$$

Uniform loading is established at the beginning of the desorption process. Hence, the first equation of Eq. (9) holds, and then the carrier containing no adsorptive component flows. Accordingly, no loading on the adsorbent surface can be assumed (the third equation).

At a certain time $t$, after desorption has started, the integrated amount of the adsorptive component $Q$ retained on a pellet is given by

$$(Q_0 - Q)/Q_0 = 1 - 6\sum_{n=1}^{\infty}(1/n^2\pi^2)\exp(-n^2\pi^2D_{app}t/a^2) \tag{10}$$

The experimental desorption curves are shown in Figs. 5 and 6. By taking the ratio $D_{app}/a^2$ as a parameter, the calculated curves were produced and fitted to the observed ones, and the final fitting curves which give the best fit to the observed ones are shown as the dashed curves in Figs. 5 and 6. It can be seen that the dashed curves and the observed ones decrease exponentially with time as predicted by Eq. (10).

Correlations of $D_{app}/a^2$ against $1/T$ are shown in Fig. 7. The data for the two different sizes are linearly correlated on a semilogarithmic scale, from which it can be deduced that transfer of the adsorptive component is limited by micropore diffusion (*5*). The present results were compared to those reported by other investigators, and they are shown in Fig. 8.

Line 1 shows the result for ethane–Linde molecular sieve 5A (particle size: 1/16 in.) reported by Antonson and Dranoff (*4*). From the result it can be deduced that the effective diffusivity shows the highest value along with the lowest activation energy, which is attributed to the fact that the molecule and micropore size are smaller and larger, respectively, than those for the present adsorption system. The molecule can move more easily than in the other cases.

Line 2 shows the result for the ethane–Linde molecular sieve 4A system reported by Kondis and Dranoff (*5*). Compared to the former case, molecule movability is depressed due to a decrease in the pore size, resulting in an increase of the activation energy.

Line 3, the present result, shows the highest activation energy and the lowest diffusivity. Differences in the molecule and pore size affect the movability.

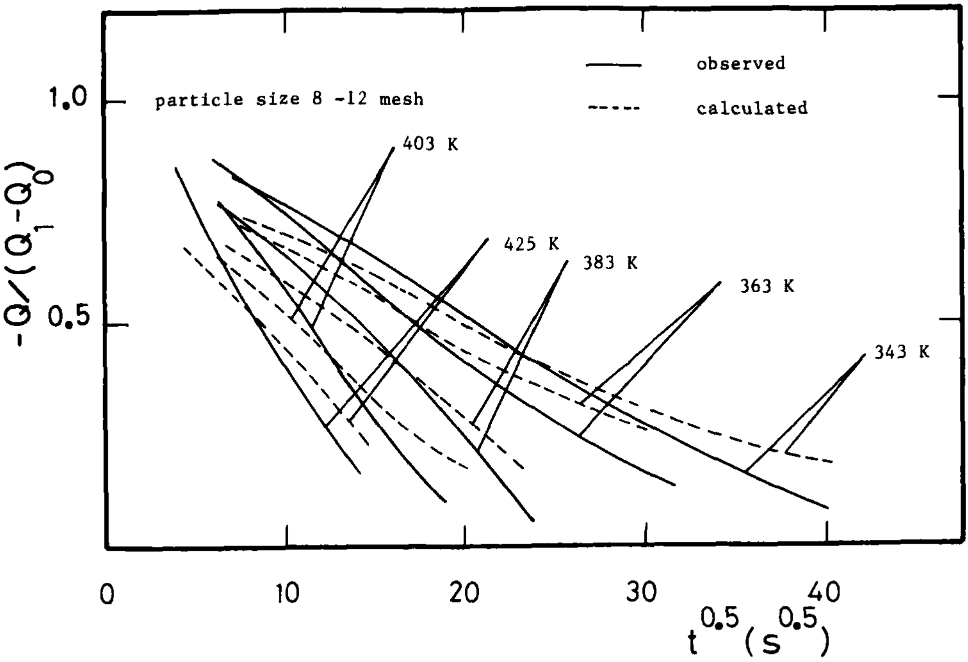

FIG. 5. The comparison of the predicted desorption curve with the observed one (8–12 mesh).

Line 4, based on Kondis and Dranoff, shows relatively low diffusivity. They stated in their article that the adsorbent contained a clay binder to reinforce its mechanical strength. Therefore, the crystal structure is not known, and sealing effects occur on the crystal surface. Owing to these two factors, the system shows a relatively low diffusivity.

In view of the above discussions, we conclude that the present results are numerically reasonable.

## CONCLUSION

A technically convenient and simple experimental method for estimating the adsorption energy during the course of the adsorption process for a gas–solid system was proposed. Also, the overall diffusion coefficient for an adsorptive species through a pellet was observed experimentally from an unsteady desorption process. The propylene gas–

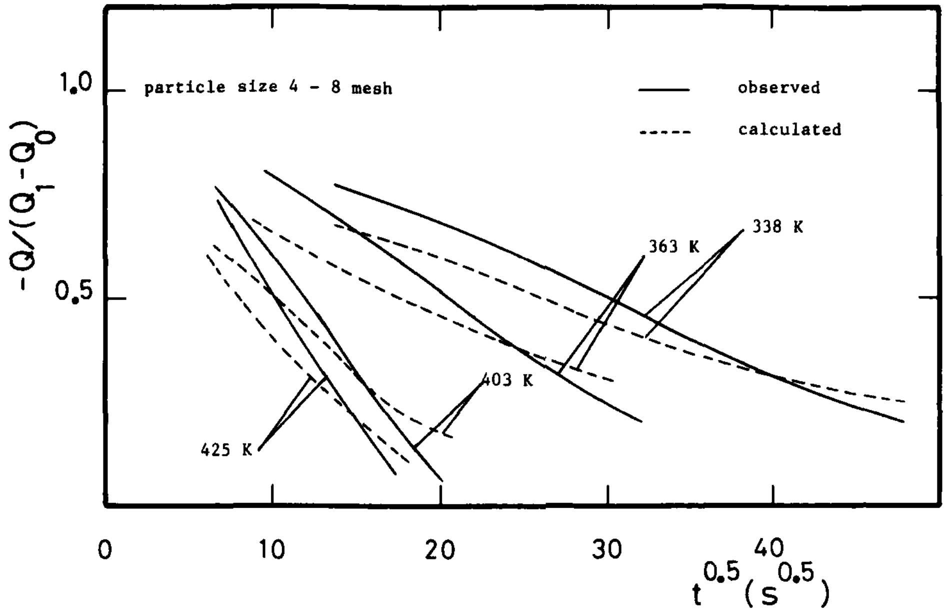

FIG. 6. The comparison of the predicted desorption curve with the observed one (4–8 mesh).

molecular sieve system was employed in this work. The adsorption energy evaluated was found to be reasonable in the light of previous work, and it was confirmed from the activation energies observed that the transfer of the adsorbable species within the molecular sieve pellet was controlled and limited by micropore diffusion.

## NOTATION

| | |
|---|---|
| $a$ | pellet radius (m) |
| $b$ | ratio between Langmuir constants ($m^3/kg$) |
| $C$ | concentration of propylene in carrier ($kg/m^3$) |
| $D_{app}$ | apparent diffusion coefficient ($m^2/s$) |
| $E_a^*$ | activation energy of adsorption (kJ/mol) |
| $E_d^*$ | activation energy of desorption (kJ/mol) |

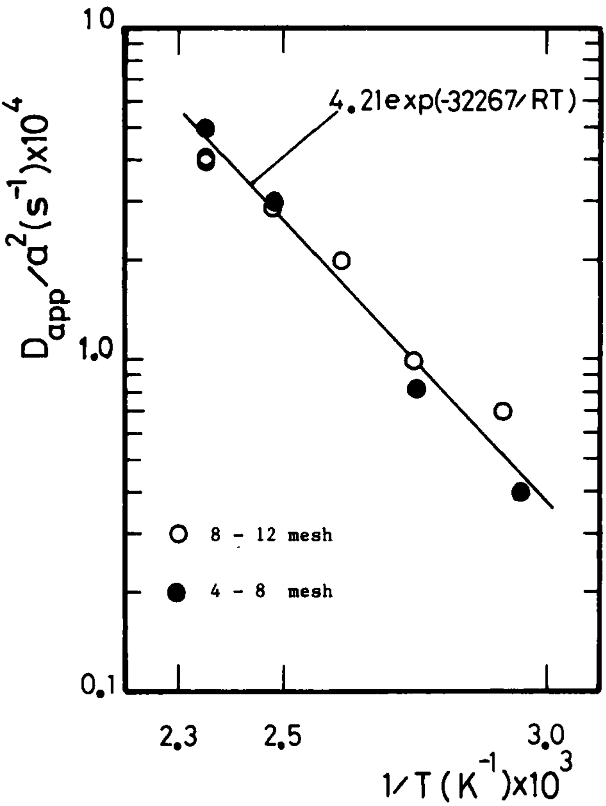

FIG. 7. The correlation of $D_{app}/a^2$ against $1/T$ to evaluate the activation energy.

| | |
|---|---|
| $k_1$ | backward rate constant (1/s) |
| $k_2$ | forward rate constant ($m^3/s \cdot kg$) |
| $Q$ | integrated adsorbed amount ($m^3/kg$) |
| | energy of adsorption (kJ/mol) |
| $Q_0$ | initial integrated loading amount ($m^3/kg$) |
| $Q_1$ | integrated loading amount at final stage of adsorption ($m^3/kg$) |
| $q$ | adsorption density ($m^3/kg$) |
| $q_{max}$ | leveling-off maximum adsorption density ($m^3/kg$) |
| $q_s$ | adsorption density at surface ($m^3/kg$) |

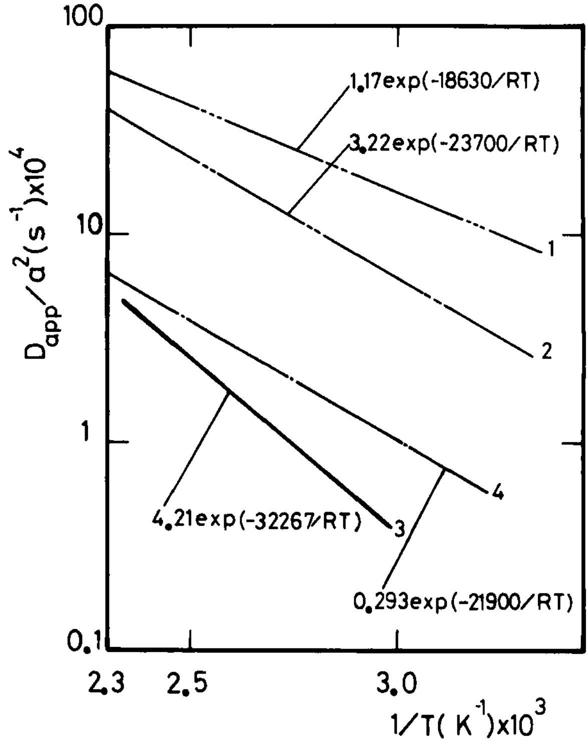

FIG. 8. Comparison of the present Arrhenius correlation with those reported by other workers.

| | |
|---|---|
| *R* | gas constant (J/mol · K) |
| *T* | absolute temperature (K) |
| *t* | time (s) |

## Greek

| | |
|---|---|
| ρ | distance from center of pellet (m) |

## REFERENCES

1. A. W. Adamson, *Physical Chemistry of Surfaces*, Wiley-Interscience, New York, 1967, Chap. 13.
2. D. M. Ruthven, D. R. Garg, and R. M. Crawford, *Chem. Eng. Sci.*, *30*, 803 (1975).

3. J. Crank, *The Mathematics of Diffusion*, Oxford University Press, Oxford, England, 1956, Chap. 6.
4. C. R. Antonson and J. S. Dranoff, *Chem. Eng. Prog. Symp. Ser.*, *65*(96), 27 (1969).
5. E. F. Kondis and J. S. Dranoff, *Ind. Eng. Chem., Process Des. Dev.*, *10*(1), 109 (1971).

*Received by editor August 26, 1988*